J Nanostruct 14(1): 232-244, Winter 2024

RESEARCH PAPER

Adsorption of Diclofenac Sodium (DS) Drug from Water on CMC-g-P(AAc-AAm) Nano-Hydrogel: Isotherm and Thermodynamic Study

Hussein Abdelamir Mohammad [1], Basam W. Mahde [2], Layth S. Jasim [3],and Maryam Batool [4]*

[1] *Pharmaceutical chemistry department, college of pharmacy, University of Al-Qadisiyah, Diwaniyah, Iraq*
[2] *College of pharmacy, University of Al-Qadisiyah, Diwaniyah, Iraq*
[3] *Department of Chemistry, College of Education, University of Al-Qadisiyah, Diwaniyah, Iraq*
[4] *Department of Chemistry, University of Sahiwal, Sahiwal, Pakistan*

ARTICLE INFO

Article History:
Received 09 April 2023
Accepted 01 May 2023
Published 01 January 2024

Keywords:
Adsorption
CMC-g-P(AAc-AAm) nano-hydrogel
Diclofenac sodium (DS) drug
Isotherm models
Thermodynamic analysis

ABSTRACT

This study deals with adsorption of a common non-steroidal anti-inflammatory drug (NSAID) i.e., diclofenac sodium (DS) using a carboxymethyl cellulose-g-poly (acrylic acid-co-acrylamide) (CMC-g-P(AAc-AAm)) nano-hydrogel. The nano-hydrogel was prepared by free-radical polymerization method and characterized by different characterization techniques including Fourier Transform Infrared Spectroscopy (FTIR), Scanning Electron Microscopy (SEM) and X-ray Diffraction (XRD) techniques. Adsorption of DS drug was investigated at its variable concentrations and temperature values. The analysis of characterization study highlights the presence of porosity and heterogenous surface of prepared nano-hydrogel. Ionic functional groups of nano-hydrogel i.e., -O-H, -N-H and -C=O were mainly involved in adsorption process. Isotherm models i.e., Langmuir, Freundlich, and Temkin models were studied that showed the fitness of data to Freundlich model with maximum adsorption capacity (q_e (mg/g)) of 1.872 mg/g. Adsorption was also studied thermodynamically that revealed the non-spontaneous and exothermic nature of the process. Overall, study suggest that the prepared nano-hydrogel has the potential to adsorb DS drug from aqueous solution with higher efficiency and removal percentage.

How to cite this article
Mohammad H., Mahde B., Jasim L., Batool M. Adsorption of Diclofenac Sodium (DS) Drug from Water on CMC-g-P(AAc-AAm) Nano-Hydrogel: Isotherm and Thermodynamic Study. J Nanostruct, 2024; 14(1):232-244. DOI: 10.22052/JNS.2024.01.024

INTRODUCTION

In today's world, pharmaceutically active compounds (PhACs) i.e., NSAIDs, antibiotics, antidepressants, and hormones appeared as an emerging water pollutant [1] that are not fully metabolized and get discharged into water. Inappropriate disposal of unused medications and inefficient working of wastewater treatment plants (WWTPs) for PhACs removal further aggravates the issue [2]. These compounds are responsible for severe health problems and environmental pollution. Among all PhACs, diclofenac sodium (DS) is one of the common non-steroidal anti-inflammatory drugs (NSAID) with numerous applications all over the world [3, 4]. This drug contains two aromatic rings and different

* *Corresponding Author Email: layth.alhayder@gmail.com*

functional groups (as phenylacetic, chlorine, secondary amino) in its structure [5]. It finds widespread uses as a cyclooxygenase inhibitor owing to its anti-inflammatory, analgesic, as well as antipyretic characteristics [6]. The remarkable proportion of this drug, however, get discharged into the environment via urine and feces. Owing to its resistant nature toward degradation, this drug stays for a longer time in water posing serious harms to aquatic life mainly fishes by damaging their kidney, gills, as well as their endocrine system. Furthermore, this is responsible for inducing oxidative stress and lowering the testosterone levels in aquatic organisms [7-15]. For mitigating the problems caused by DS drug pollution, there is a need for developing some effective water treatment methods aiming to remove DS drug from wastewater and industrial effluents to reduce its associated health risks both to humans and environment [8, 15-17].

Different procedures for treating polluted water have been developed as advanced oxidation, membrane filtration, membrane-sorption hybrids and adsorption. Among these techniques, adsorption process is widely employed method due to its low energy consumption, easy operation, and high effectiveness [18-30]. In adsorption process, selecting the most appropriate adsorbent is the crucial step and numerous adsorbents have been developed till date. Hydrogels are widely used adsorbents owing to their hydrophilic nature, large surface area available for adsorption and diversity of functional groups in its structure [31, 32]. These materials are biocompatible and biodegradable in nature [33-35]. Sodium carboxymethyl cellulose (CMC) is a polymer that finds extensive uses in different fields mainly due to its unique chemical, physical, and biological characteristics. Presence of amine (-NH_2) and carboxyl (-COOH) functional groups in CMC make it pH sensitive as its swelling is more in basic solutions rather than in acidic ones. This property of CMC make it effective adsorbing material for controlled drug delivery systems [36].

However, to further improve the adsorbing potential of CMC, different polymers are grafted in it. Poly acrylic acid (PAAc) and polyacrylamide (PAAm) possess high efficiency for adsorbing variety of pollutants [37] mainly due to presence of ionic functional groups in their structure [38, 39]. This study deals with use of carboxymethyl cellulose-g-poly (acrylic acid-co-acrylamide) i.e., CMC-g-P(AAc-AAm) nano-hydrogel for adsorptive removal of DS drug from water. The adsorbent's synthesis was done by method of free radical polymerization and further analyzed via FTIR, SEM and XRD. Adsorption of drug was studied at variable temperatures and concentrations. Data from adsorption study was applied to Langmuir, Freundlich and Temkin models for describing the adsorption mechanism. The thermodynamic behaviour of DS drug adsorption on prepared nano-hydrogel was also analyzed by applying Van't Hoff plot. Findings revealed adsorptive potential of prepared adsorbent toward DS drug adsorption.

MATERIALS AND METHODS

Reagents and chemicals

The reagents used in current study were sodium carboxmethyl cellulose (NaCMC, $C_{28}H_{30}Na_8O_{27}$), acrylamide (AAm, C_3H_5NO), N, N'-methylene-bis-acrylamide (MBA, $C_7H_{10}N_2O_2$) and Mueller-Hinton agar that were procured from Himedia. Furthermore, potassium per sulfate (KPS, $K_2S_2O_8$) and sodium chloride (NaCl) were obtained from Fluka. From Thomas maker, acrylic acid (AAc, $C_3H_4O_2$) and from Alpha Chemika, potassium chloride (KCl) were purchased. Additionally, from B.D.H, hydrochloric acid (HCl) was obtained. Nitrogen gas (N_2) was also used in study. The purity percentages of these chemicals vary, but most of them have purity greater than 98%.

Preparation of CMC-g-P(AAc-AAm) nano-hydrogel

To synthesize CMC-g-P(AAc-AAm), free radical polymerization method was used. Potassium persulfate (KPS) was utilized as an initiator while methylene bisacrylamide (MBA) served as a crosslinking agent. Initially, 1g of sodium carboxymethyl cellulose (CMC) was dissolved in 20 mL deionized distilled water in a three-necked round-bottom flask that was equipped with a condenser, separating funnel, and nitrogen gas inlet. This was followed by heating the solution with continuous stirring in a magnetic stirrer-heater maintained at temperature of 50 °C till a homogeneous and transparent solution was obtained. Cooling of solution was carried out at normal temperature. In the next step, the initiator solution (0.1g KPS in 2 mL water) was added to above solution with stirring using separating funnel. Subsequently, an acrylamide (AAm) solution (1g AAm in 1 mL of deionized distilled water) was introduced in above mixture with constant stirring followed by addition of 4 mL

acrylic acid (AAc) with ongoing stirring. Next, the crosslinker solution of MBA (0.05g MBA in 1 mL deionized distilled water) was added, ensuring thorough mixing. All additions were performed under a nitrogen (N_2) atmosphere. Finally, mixture was added to test tubes and placed in a water bath at 70°C for time period of two hours that allow the formation of nano-hydrogel [40, 41] as depicted in Fig. 1.

Activating the surface of prepared nano-hydrogel and characterization study

The prepared nano-hydrogel was cut into small pieces followed by washing with deionized distilled water for one hour. The washing process was repeated several times to remove any unreacted materials. After thorough washing, the nano-hydrogel was dried at 60°C and subsequently ground to small particles (Fig. 2).

Successful synthesis of nano-hydrogel was confirmed by its analysis via different techniques namely Fourier Transform Infrared (FTIR, Shimadzu 8400s spectrophotometer from 500 to 4000 cm^{-1}), Field Emission Scanning Electron Microscopy (FESEM, TESCAN MIRA3 at voltage of 25 kV) and X-ray Diffraction (XRD, Shimadzu XRD-6000, with 2θ range of 10° to 80°).

Calibration curve and adsorption study

For plotting the calibration curve, variable solutions of DS drug (1 mg/L to 30 mg/L) prepared and measurement of absorbance was carried out.

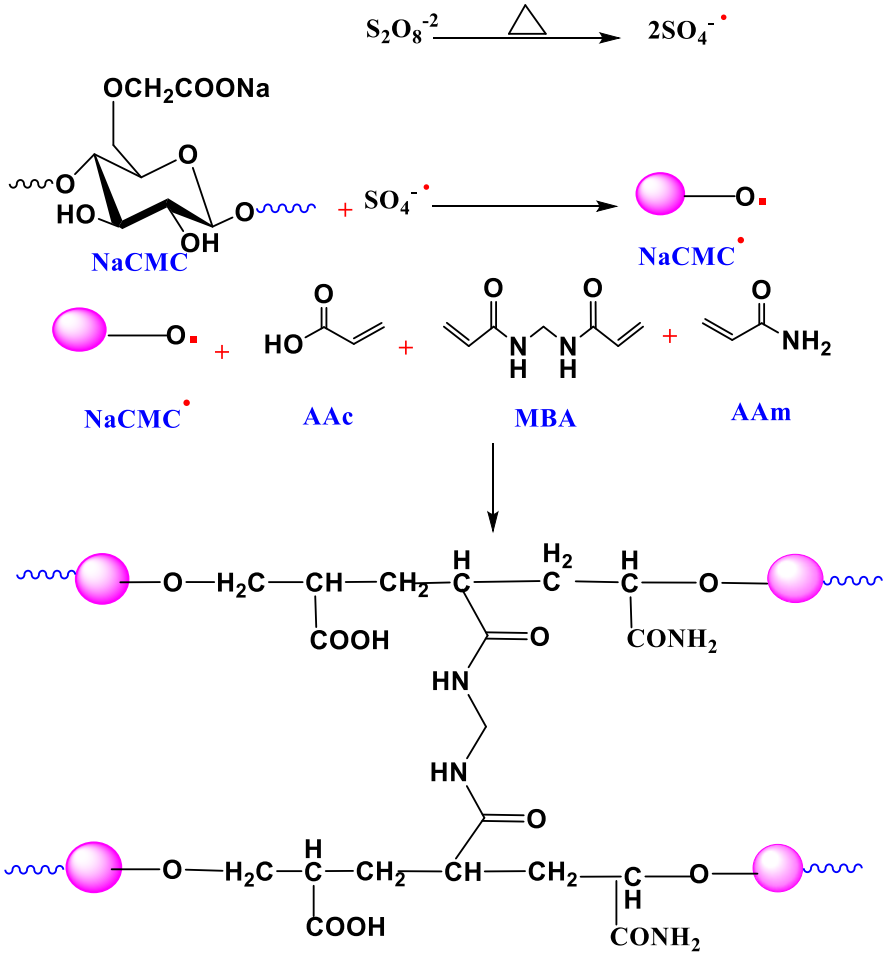

Fig. 1. Free radical polymerization method for nano-hydrogel synthesis.

Results of calibration graph (Fig. 3) revealed the higher correlation coefficient value highlighting linear relation between drug concentration and its respective absorbance.

For studying the adsorption of DS drug from water, solutions of variable concentrations were prepared varying from 10 mg/L to 180 mg/L at variable temperatures i.e., from 10 °C to 30 °C. All experiments were performed at solution pH of 9 and shaking speed of 120 rpm. The amount of nano-hydrogel used in each experiment was 0.06g. After an equilibrium time of 120 min, adsorption efficiency calculation was carried out employing Eq. 1:

$$q_e = \frac{C_0 - C_e}{M} \times V \quad (1)$$

Here C_0 and C_e, V (mL) and M (g) denotes initial, equilibrium dye concentrations (mg/l), solution volume and weight of adsorbent correspondingly. Three isotherm models i.e., Langmuir, Freundlich, Temkin were studied to better understand mechanism of adsorption. While results from

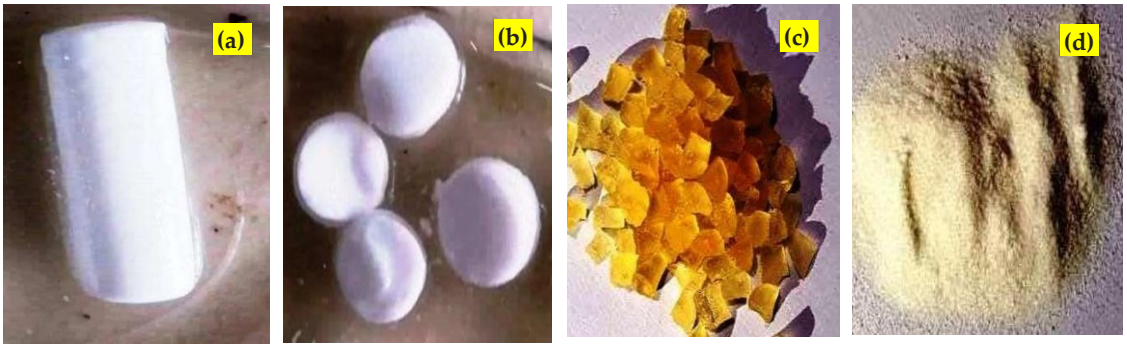

Fig. 2. Images of prepared nano-hydrogel after (a) cutting, (b) washing, (c) drying and (d) grinding.

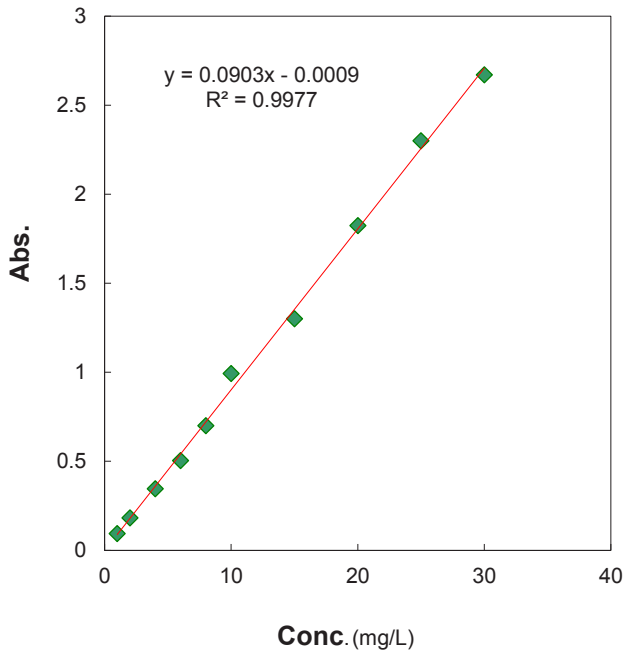

Fig. 3. Calibration curve for DS drug.

experiment of temperature study were analyzed by applying thermodynamic model highlighting the feasibility of process.

RESULTS AND DISCUSSION

Characterization results

The functional group study of nano-hydrogel

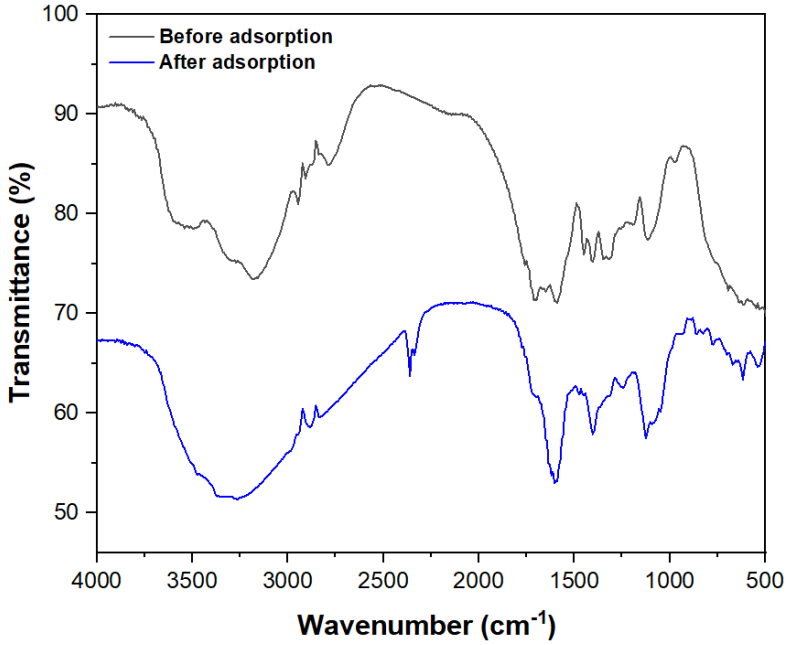

Fig. 4. FTIR results of prepared nano-hydrogel both before and after drug adsorption.

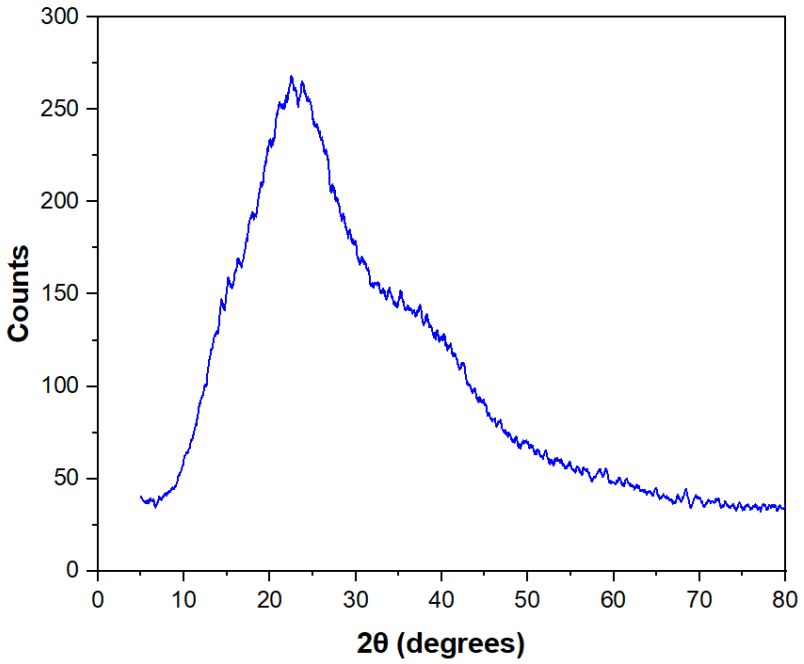

Fig. 5. XRD results of prepared nano-hydrogel.

(Fig. 4) revealed the presence of numerous functional groups in it. The peak obtained within range 3600-3100 cm^{-1} correspond to the presence of -N-H and -O-H stretching vibrations while the -C-H stretching vibrations were observed by the presence of small peaks from 2900 cm^{-1} to 2800 cm^{-1}. Peaks at 1720 cm^{-1} and 1630 cm^{-1} to 1560 cm^{-1} are mainly due to the vibrations of -C=O bonds in acrylic acid (AAc) and acrylamide (AAm) respectively. In addition to that, asymmetric and symmetric stretching vibrations of -C=O in carboxylate ions are observed by the peaks at 1488 cm^{-1} and 1380 cm^{-1} correspondingly. Peak obtained at 1164 cm^{-1} and 995 cm^{-1} corresponds mainly to the presence of -C-N and -C-O-C bond vibrations correspondingly. Post adsorption analysis of FTIR revealed remarkable change in both intensity and position of -N-H, -O-H, -C=O, -C-N and -C-O-C peaks obtained. This reflects the interactions between functional groups of studied nano-hydrogel and adsorbed drug molecules [17, 36, 42-52].

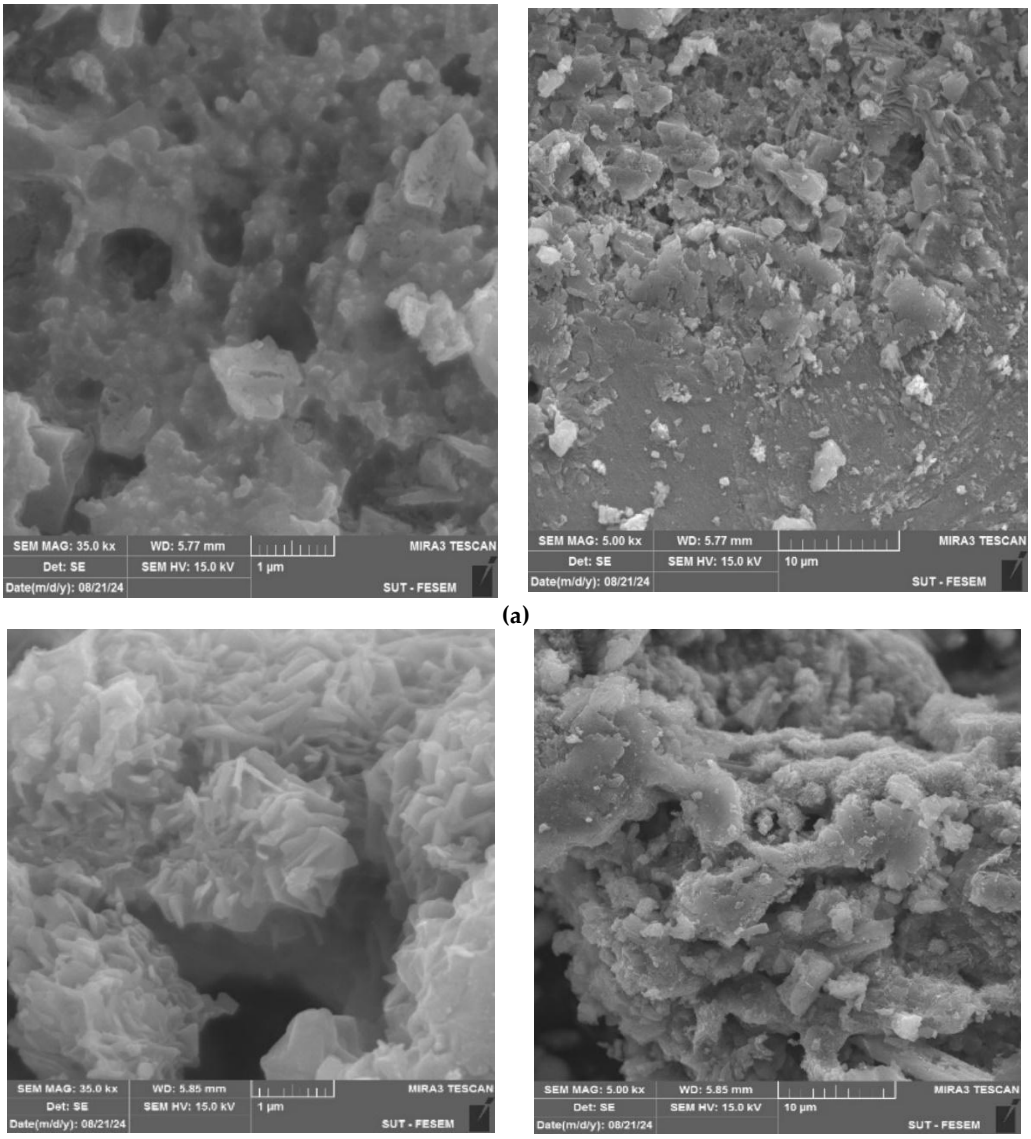

Fig. 6. FESEM results of prepared nano-hydrogel (a) before and (b) after drug adsorption.

Crystallographic results of XRD (Fig. 5) revealed the presence of a broad peak i.e., at 2θ = 20° to 30°. This peak confirmed the amorphous nature of prepared nano-hydrogel i.e., absence of long-range order and less crystallinity that is one of the key properties of majority of hydrogels due to presence of inter-linked polymers in it. This amorphous nature of nano-hydrogel is responsible for its high swelling property i.e., high water retention ability that aid in effective drug adsorption [36].

Morphological analysis of prepared nano-hydrogel revealed the presence of numerous pores and heterogeneity on its surface before drug adsorption (Fig. 6a). The presence of heterogeneity is the key feature for any adsorbent. The small size particles of nano-hydrogel are responsible for adsorbing drug molecules on its surface [53]. Post adsorption FESEM results (Fig. 6b) revealed the conversion of heterogeneous surface to somewhat homogeneous surface due to filling of empty active sites by drug molecules. In summary,

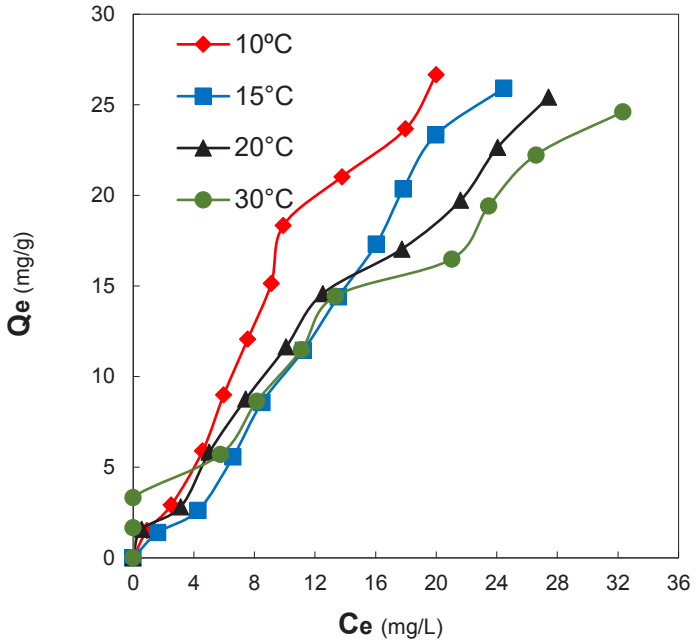

Fig. 7. Adsorption of drug onto prepared nano-hydrogel at variable temperatures.

Table 1. Effect of drug concentration on adsorption capacity (mg/g) of adsorbent at variable temperatures.

C_o (mg/L)	10 °C		15 °C		20 °C		30 °C	
	C_e (mg/L)	q_e (mg/g)	C_e (mg/L)	q_e (mg/g)	C_e (mg/L)	q_e (mg/g)	C_e (mg/L)	q_e (mg/g)
0	0	0	0	0	0	0	0	0
10	0.918051	1.513658	1.6268	1.395533	0.563677	1.572721	0	1.666667
20	2.512735	2.914544	4.284607	2.619232	3.13289	2.811185	0	3.333333
40	4.58361	5.902732	6.58804	5.56866	5.026578	5.828904	5.757475	5.707087
60	5.978959	9.003507	8.503876	8.582687	7.429679	8.76172	8.160576	8.639904
80	7.562569	12.07291	11.2392	11.46013	10.09856	11.65024	11.10631	11.48228
100	9.112957	15.14784	13.54264	14.40956	12.51274	14.58121	13.3433	14.44278
120	9.910299	18.34828	16.05648	17.32392	17.73976	17.04337	21.02879	16.4952
140	13.78627	21.03562	17.82835	20.36194	21.61573	19.73071	23.47619	19.42063
160	17.98339	23.66944	19.97674	23.33721	24.06312	22.65615	26.58804	22.23533
180	20.00997	26.66501	24.46179	25.92303	27.42968	25.42839	32.32447	24.61259

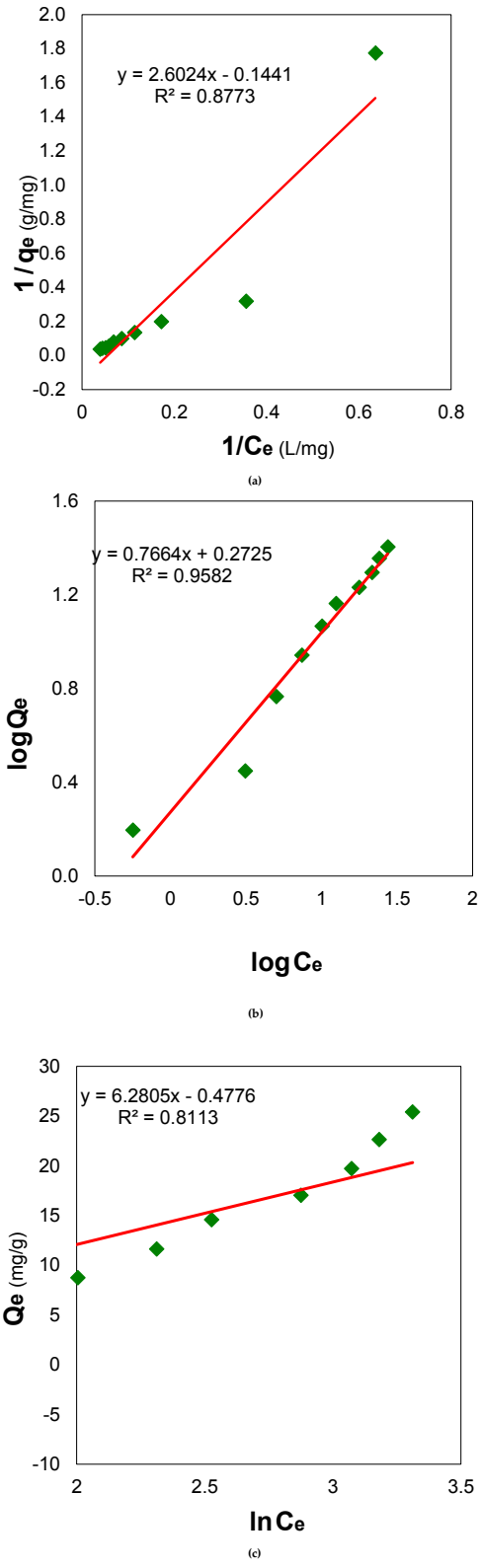

Fig. 8. Graph of (a) Langmuir, (b) Freundlich, (c) Temkin model for drug adsorption on prepared nano-hydrogel.

the surface characteristics of nano-hydrogel varied after drug adsorption due to interactions taking place between drug molecules and surface of nano-hydrogel [21, 36, 54-57].

Isotherm and thermodynamic study

Effect of drug concentration on adsorption capacity of prepared nano-hydrogel was studied at variable concentrations and temperatures. Results of study (Fig. 7 and Table 1) showed that an increase in solution concentration led to an increase in adsorption capacity while on the other hand, increasing temperature resulted in decrement in adsorption capacity (Q_e). Maximum adsorption can take place at the highest concentration i.e., 180 mg/L but at the lowest temperature i.e., 10

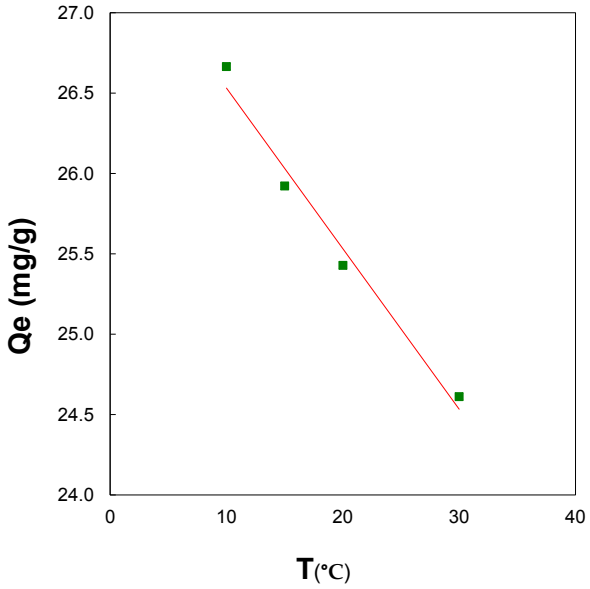

Fig. 9. Influence of temperature on drug adsorption onto the prepared nano-hydrogel.

Table 2. Langmuir, Freundlich and Temkin model parameters.

Langmuir	Freundlich	Temkin
q_0 (mg/ g)	K_f (mg g^{-1})	B (J/mol)
-6.93	1.872	6.28
b (L/g)	1/ n	A_T (L/g)
-0.055	0.503	0.926
	R^2	
0.8773	0.9582	0.8113

Table 3. Influence of temperature for drug adsorption onto prepared nano-hydrogel in terms of q_e (mg/g).

Temperature (°C)	q_e (mg/g)
10	26.66501
15	25.92303
20	25.42839
30	24.61259

°C where 26.66 mg of drug adsorbed per gram of adsorbent surface. This capacity continues to decrease with increase in temperature and reaches 24.61 mg/g while using 180 mg/L solution at 30 °C. The results are further confirmed by the thermodynamic study wherein the value of enthalpy change was negative highlighting the exothermic nature of adsorption. This can be attributed to the weakening of attractive forces between studied drug molecules and adsorbent surface at higher temperatures [58].

Data from concentration study was applied to different isotherm models. The Langmuir model mainly deals with single layer adsorption of pollutant on adsorbing material [18]. Freundlich isotherm, on the other hand, involves the adsorption of pollutant on adsorbent surface in multilayer manner [25]. For better understanding of interactions taking place between adsorbent and the adsorbate, Temkin model is widely employed that provides information regarding adsorption heat changes taking place throughout the adsorption process [59]. Linearized forms of Langmuir, Freundlich as well as Temkin model are expressed by Eqs. 2, 3 and 4 correspondingly.

$$\frac{1}{q_e} = \frac{1}{q_{max}} + \frac{1}{q_o b C_e} \quad (2)$$

The Langmuir constant and maximum adsorption capacity are represented by b (L/mg) and q_{max} (mg/g) correspondingly.

$$\log q_e = \log K_f + \frac{1}{n} \log C_e \quad (3)$$

Constant and exponent of Freundlich model (mg/g) are represented by k_f and 'n' correspondingly [56].

$$q_{eq} = B \ln A_T + B \ln C_{eq} \quad (4)$$

here, and B refers to constant of universal gas (J/mol K) and adsorption heat (J/mol), , and refers to constant of Temkin equilibrium binding

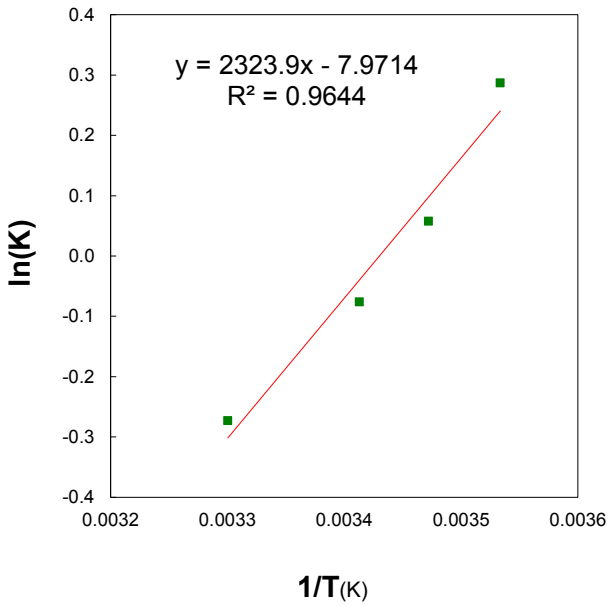

Fig. 10. Van't Hoff graph.

Table 4. Parameters obtained from Van't Hoff graph.

T (°C)	ΔG (kJ/mol)	ΔH (kJ/mol)	ΔS (J/mol K)	K_c
20	0.185	-19.321	-66.274	0.927

(L/ g), Temkin constant (J/ mol) and absolute temperature in Kelvin correspondingly [59]. Results (Fig. 8a-c and Table 2) revealed that data fits best to Freundlich model that has the highest regression coefficient value i.e., 0.9582 when compared with Langmuir (R^2 = 0.8773) and Temkin (R^2 = 0.8113) models. Furthermore, data revealed the maximum adsorption capacity of 1.872 mg/g from Freundlich model revealing the multilayer adsorption of drug on heterogenous adsorbent surface [58].

Effect of temperature on adsorption capacity of adsorbent was investigated by varying temperature from 10 °C to 30 °C for 500 mg/L drug concentration solution for an equilibrium time of 120 min. Results (Fig. 9 and Table 3) revealed that with increasing temperature, adsorption capacity of adsorbent for drug adsorption decreases continuously. With increasing temperature from 10 °C to 30 °C, there was a decrement in adsorption capacity from 26.66 mg/g to 24.61 mg/g respectively. Findings showed exothermic nature of process suggesting breakdown of weak adsorption forces (van der Waals forces or dipole-dipole interactions) between drug molecules and adsorbent surface at higher temperatures [58].

Data from temperature study was analyzed thermodynamically for examining the feasibility of process in terms of thermodynamic parameters (i.e., ΔH, ΔS, and ΔG). For calculating value of ΔG (Eq. 5), distribution coefficient, k_c, was employed (Eq. 6):

$$\Delta G = -RT \ln k_c \quad (5)$$

$$k_c = \frac{C_{ad}}{C_e} \quad (6)$$

where C_{ad} (mg/L), R , T denotes to drug concentration that get adsorbed, ideal gas constant (8.314 J/mol K) and absolute temperature in Kelvin correspondingly. For calculating the change in Gibbs free energy (ΔG), Eq. 7 can be used:

$$\Delta G = \Delta H - T\Delta S \quad (7)$$

When we substitute Equation (5) into Equation (7), an expression for ln k_c can be obtained as Eq. 8:

$$\ln k_c = -\frac{\Delta H}{RT} + \frac{\Delta S}{R} \quad (8)$$

From the graph (Van't Hoff graph) plotted between ln (K_c) and 1/T, values of ΔH and ΔS were determined from its slope and intercept, correspondingly. Results of Van't Hoff plot are shown in Fig. 10 and parameters calculated from its slope and intercept are elaborated in Table 4. Data revealed the non-spontaneous and exothermic behaviour of process due to positive and negative values obtained for ΔG and ΔH respectively. Furthermore, study revealed the decreased randomness of system with increasing temperature revealing feasibility of studied process [60, 61].

CONCLUSION

This research was devoted to investigate the adsorptive potential of CMC-g-P(AAc-AAm) nano-hydrogel towards diclofenac sodium (DS) drug removal from water. The nano-hydrogel synthesis was carried out via free radical polymerization method and characterized by different techniques namely FTIR, SEM, and XRD. The analysis revealed the highly porous, heterogenous adsorbent surface that possess numerous ionic functional groups favoring the adsorption process. Concentration study showed fitness of data to Freundlich model suggesting multilayer adsorption with maximum adsorption capacity of 1.872 mg/g. From temperature study, feasibility of the process and higher adsorption capacity at the lowest temperature was confirmed. Overall, the study revealed the potential of prepared adsorbent for DS drug adsorption from water.

CONFLICT OF INTEREST

The authors declare that there is no conflict of interests regarding the publication of this manuscript.

REFERENCES

1. Patel M, Kumar R, Kishor K, Mlsna T, Pittman CU, Mohan D. Pharmaceuticals of Emerging Concern in Aquatic Systems: Chemistry, Occurrence, Effects, and Removal Methods. Chemical Reviews. 2019;119(6):3510-3673.
2. Glassmeyer ST, Hinchey EK, Boehme SE, Daughton CG, Ruhoy IS, Conerly O, et al. Disposal practices for unwanted residential medications in the United States. Environment International. 2009;35(3):566-572.
3. Salvestrini S, Fenti A, Chianese S, Iovino P, Musmarra D. Diclofenac sorption from synthetic water: Kinetic and thermodynamic analysis. Journal of Environmental Chemical Engineering. 2020;8(5):104105.
4. Kozlowska M, Rodziewicz P, Kaczmarek-Kedziera A. Structural stability of diclofenac vs. inhibition activity from ab initio molecular dynamics simulations. Comparative

study with ibuprofen and ketoprofen. Structural Chemistry. 2017;28(4):999-1008.
5. He B-s, Wang J, Liu J, Hu X-m. Eco-pharmacovigilance of non-steroidal anti-inflammatory drugs: Necessity and opportunities. Chemosphere. 2017;181:178-189.
6. Verlicchi P, Al Aukidy M, Zambello E. Occurrence of pharmaceutical compounds in urban wastewater: Removal, mass load and environmental risk after a secondary treatment—A review. Science of The Total Environment. 2012;429:123-155.
7. Guiloski IC, Ribas JLC, Pereira LdS, Neves APP, Silva de Assis HC. Effects of trophic exposure to dexamethasone and diclofenac in freshwater fish. Ecotoxicology and Environmental Safety. 2015;114:204-211.
8. Shamsudin MS, Azha SF, Sellaoui L, Badawi M, Bonilla-Petriciolet A, Ismail S. Performance and interactions of diclofenac adsorption using Alginate/Carbon-based Films: Experimental investigation and statistical physics modelling. Chemical Engineering Journal. 2022;428:131929.
9. Mahmood Taher A, Ali Kadhim Kyhoiesh H, Shakir Waheeb A, Al-Adilee KJ, Jasim LS. Synthesis, characterization, biological activity, and modelling protein docking of divalent, trivalent, and tetravalent metal ion complexes of new azo dye ligand (N,N,O) derived from benzimidazole. Results in Chemistry. 2024;12:101911.
10. The value of two onset determination of anti-H.pylori IgM antibody in patients with dyspepsia in Iraq. International Journal of Pharmaceutical Research. 2020;12(02).
11. Bayati-Komitaki N, Ganduh SH, Alzaidy AH, Salavati-Niasari M. A comprehensive review of Co3O nanostructures in cancer: Synthesis, characterization, reactive oxygen species mechanisms, and therapeutic applications. Biomedicine and Pharmacotherapy. 2024;180:117457.
12. The value of iron supplementation to children with Helicobacter pylori infection in Iraq: a cross-sectional study. International Journal of Pharmaceutical Research. 2020;12(02).
13. Çetin M, Ozudogru Y. Removal of malachite green dye by adsorption onto chitosan-montmorillonite nanocomposite: Kinetic, thermodynamic and equilibrium studies. Journal of the Chinese Chemical Society. 2025.
14. Mittal H, Al Alili A, Alhassan SM. High efficiency removal of methylene blue dye using κ-carrageenan-poly(acrylamide-co-methacrylic acid)/AQSOA-Z05 zeolite hydrogel composites. Cellulose. 2020;27(14):8269-8285.
15. Kanwal F, Javed T, Hussain F, Wasim M, Batool M. Enhanced dye photodegradation through ZnO and ZnO-based photocatalysts doped with selective transition metals: a review. Environmental Technology Reviews. 2024;13(1):754-793.
16. Tatarchuk T, Myslin M, Lapchuk I, Shyichuk A, Murthy AP, Gargula R, et al. Magnesium-zinc ferrites as magnetic adsorbents for Cr(VI) and Ni(II) ions removal: Cation distribution and antistructure modeling. Chemosphere. 2021;270:129414.
17. Saadallah K, Ad C, Djedid M, Batool M, Benalia M, Saadallah S, Hamamda S. Potential of the Algerian pine tree bark for the adsorptive removal of methylene blue dye: Kinetics, isotherm and mechanism study. Journal of Dispersion Science and Technology. 2024:1-19.
18. Batool M, Javed T, Wasim M, Zafar S, Din MI. Exploring the usability of Cedrus deodara sawdust for decontamination of wastewater containing crystal violet dye. Desalination and Water Treatment. 2021;224:433-448.
19. Ghzal Q, Javed T, Batool M. Potential of easily prepared low-cost rice husk biochar and burnt clay composite for the removal of methylene blue dye from contaminated water. Environmental Science: Water Research & Technology. 2023;9(11):2925-2941.
20. Majeed HJ, Idrees TJ, Mahdi MA, Abed MJ, Batool M, Yousefi SR, et al. Synthesis and application of novel sodium carboxy methyl cellulose-g-poly acrylic acid carbon dots hydrogel nanocomposite (NaCMC-g-PAAc/ CDs) for adsorptive removal of malachite green dye. Desalination and Water Treatment. 2024;320:100822.
21. Mannan HA, Nadeem R, Bibi S, Javed T, Javed I, Nazir A, et al. Mesoporous activated TiO_2 based biochar synthesized from fish scales as a proficient adsorbent for deracination of heavy metals from industrial efflux. Journal of Dispersion Science and Technology. 2022;45(2):329-341.
22. Shah A, Arjunan A, Manning G, Batool M, Zakharova J, Hawkins AJ, et al. Sequential novel use of Moringa oleifera Lam., biochar, and sand to remove turbidity, E. coli, and heavy metals from drinking water. Cleaner Water. 2024;2:100050.
23. Shah A, Arjunan A, Thumma A, Zakharova J, Bolarinwa T, Devi S, Batool M. Adsorptive removal of arsenic from drinking water using KOH-modified sewage sludge-derived biochar. Cleaner Water. 2024;2:100022.
24. Shah A, Zakharova J, Batool M, Coley MP, Arjunan A, Hawkins AJ, et al. Removal of cadmium and zinc from water using sewage sludge-derived biochar. Sustainable Chemistry for the Environment. 2024;6:100118.
25. Bukhari A, Javed T, Haider MN. Adsorptive exclusion of crystal violet dye from wastewater by using fish scales as an adsorbent. Journal of Dispersion Science and Technology. 2022;44(11):2081-2092.
26. Imran MS, Javed T, Areej I, Haider MN. Sequestration of crystal violet dye from wastewater using low-cost coconut husk as a potential adsorbent. Water Science and Technology. 2022;85(8):2295-2317.
27. Urooj H, Javed T, Taj MB, Nouman Haider M. Adsorption of crystal violet dye from wastewater on Phyllanthus emblica fruit (PEF) powder: kinetic and thermodynamic. International Journal of Environmental Analytical Chemistry. 2023;104(19):7474-7499.
28. Arshad R, Javed T, Thumma A. Exploring the efficiency of sodium alginate beads and Cedrus deodara sawdust for adsorptive removal of crystal violet dye. Journal of Dispersion Science and Technology. 2023;45(12):2330-2343.
29. Javed T, Thumma A, Uddin AN, Akhter R, Babar Taj M, Zafar S, et al. Batch adsorption study of Congo Red dye using unmodified Azadirachta indica leaves: isotherms and kinetics. Water Practice & Technology. 2024;19(2):546-566.
30. Rehman H, Javed T, Thumma A, Uddin AN, Singh N, Baig MM, et al. Potential of easily available low-cost raw cotton for the elimination of methylene blue dye from polluted water. Desalination and Water Treatment. 2024;318:100319.
31. Okesola BO, Smith DK. Applying low-molecular weight supramolecular gelators in an environmental setting – self-assembled gels as smart materials for pollutant removal. Chemical Society Reviews. 2016;45(15):4226-4251.
32. Seida Y, Tokuyama H. Hydrogel Adsorbents for the Removal of Hazardous Pollutants-Requirements and Available Functions as Adsorbent. Gels (Basel, Switzerland). 2022;8(4):220.
33. Ekiz MS, Cinar G, Khalily MA, Guler MO. Self-assembled peptide nanostructures for functional materials.

Nanotechnology. 2016;27(40):402002.
34. Levin A, Hakala TA, Schnaider L, Bernardes GJL, Gazit E, Knowles TPJ. Biomimetic peptide self-assembly for functional materials. Nature reviews Chemistry. 2020;4(11):615-634.
35. Edwards-Gayle CJC, Hamley IW. Self-assembly of bioactive peptides, peptide conjugates, and peptide mimetic materials. Organic & Biomolecular Chemistry. 2017;15(28):5867-5876.
36. Faleh YA, Radhy ND. Removal of Metformin hydrochloride from Aqueous Solutions by using Carboxymethyl cellulose-g-poly(acrylic acid-co-acrylamide) Hydrogel: Adsorption and Thermodynamic Studies. IOP Conference Series: Earth and Environmental Science. 2021;790(1):012062.
37. Xu B, Zheng C, Zheng H, Wang Y, Zhao C, Zhao C, Zhang S. Polymer-grafted magnetic microspheres for enhanced removal of methylene blue from aqueous solutions. RSC Adv. 2017;7(74):47029-47037.
38. Tang Y, He T, Liu Y, Zhou B, Yang R, Zhu L. Sorption behavior of methylene blue and rhodamine B mixed dyes onto chitosan graft poly (acrylic acid-co-2-acrylamide-2-methyl propane sulfonic acid) hydrogel. Advances in Polymer Technology. 2018;37(7):2568-2578.
39. Lebkiri I, Abbou B, Kadiri L, Ouass A, Essaadaoui Y, Ouaddari H, et al. Polyacrylamide Hydrogel an Effective Adsorbent for the Removal of Heavy Metal from Aqueous Solution: Isotherm, Kinetic, and Thermodynamic Studies. Russian Journal of Physical Chemistry A. 2022;96(7):1484-1492.
40. Dai H, Huang H. Enhanced Swelling and Responsive Properties of Pineapple Peel Carboxymethyl Cellulose-g-poly(acrylic acid-co-acrylamide) Superabsorbent Hydrogel by the Introduction of Carclazyte. Journal of Agricultural and Food Chemistry. 2017;65(3):565-574.
41. Radwan EK, Kafafy H, El-Wakeel ST, Shaheen TI, Gad-Allah TA, El-Kalliny AS, El-Naggar ME. Remediation of Cd(II) and reactive red 195 dye in wastewater by nanosized gels of grafted carboxymethyl cellulose. Cellulose. 2018;25(11):6645-6660.
42. Studies on Removal of Methylene Blue Dye from Aqueous Solution by Adsorption Using Low Cost Adsorbent. Knowledge of Research. 2016.
43. Moussa I, Khiari R, Moussa A, Belgacem MN, Mhenni MF. Preparation and Characterization of Carboxymethyl Cellulose with a High Degree of Substitution from Agricultural Wastes. Fibers and Polymers. 2019;20(5):933-943.
44. Leshaf A, Ziani Cherif H, Benmansour K. Adsorption of Acidol Red 2BE-NW Dye from Aqueous Solutions on Carboxymethyl Cellulose/Organo-Bentonite Composite: Characterization, Kinetic and Thermodynamic Studies. Journal of Polymers and the Environment. 2019;27(5):1054-1064.
45. Razavi FS, Mahdi MA, Ghanbari D, Dawi EA, Abed MJ, Ganduh SH, et al. Fabrication and design of four-component Bi_2S_3/$CuFe_2O_4$/CuO/Cu_2O nanocomposite as new active materials for high performance electrochemical hydrogen storage application. Journal of Energy Storage. 2024;94:112493.
46. Kareem NS, Mohammed SA, Abed MJ, Aneed AH, Kamal HM, Zahid NI, Sabah KJ. New macrocycles incorporating glycolipids via copper-catalyzed triazole coupling. Journal of Carbohydrate Chemistry. 2022;41(1):1-17.
47. Chen T, Wong Y-S. Selenocystine induces reactive oxygen species–mediated apoptosis in human cancer cells. Biomedicine & Pharmacotherapy. 2009;63(2):105-113.
48. Yasir AF, Jamel HO. Synthesis of a New DPTYEAP Ligand and Its Complexes with Their Assessments on Physical Properties, Antioxidant, and Biological Potential to Treat Breast Cancer. Indonesian Journal of Chemistry. 2023;23(3):796.
49. Hosseini M, Ghanbari M, Dawi EA, Mahdi MA, Ganduh SH, Jasim LS, et al. Investigations of nickel silicate for degradation of water-soluble organic pollutants. International Journal of Hydrogen Energy. 2024;61:307-315.
50. Batool M, Haider MN, Javed T. Applications of Spectroscopic Techniques for Characterization of Polymer Nanocomposite: A Review. Journal of Inorganic and Organometallic Polymers and Materials. 2022;32(12):4478-4503.
51. Shah A, Arjunan A, Manning G, Zakharova J, Andraulaki I, Batool M. The effect of dose, settling time, shelf life, storage temperature and extractant on Moringa oleifera Lam. protein coagulation efficiency. Environmental Nanotechnology, Monitoring & Management. 2024;21:100919.
52. Shah A, Manning G, Zakharova J, Arjunan A, Batool M, Hawkins AJ. Particle size effect of Moringa oleifera Lam. seeds on the turbidity removal and antibacterial activity for drinking water treatment. Environmental Chemistry and Ecotoxicology. 2024;6:370-379.
53. Pang YL, Tee SF, Limg S, Abdullah AZ, Ong HC, Wu C-H, et al. Enhancement of photocatalytic degradation of organic dyes using ZnO decorated on reduced graphene oxide (rGO). Desalination and Water Treatment. 2018;108:311-321.
54. Akhlaq M, Naz S, Uroos M. Facile fabrication of high capacity citric acid cross-linked chitosan and carboxymethyl cellulose-based hydrogel for fast kinetics removal of Cu(II). Adsorption. 2024;30(3-4):363-375.
55. Javed T, Kausar F, Zawar MD, Khalid N, Thumma A, Ismail A, et al. Investigating the adsorption potential of coconut coir as an economical adsorbent for decontamination of lanthanum ion from aqueous solution. Journal of Dispersion Science and Technology. 2024:1-12.
56. Ayni S, Sabet M, Mahdi MA, Abdulsahib WK, Taher AM, Zareie N, Salavati-Niasari M. Synthesis of flower-like and hexagonal PbWO4 nanostructures via the co-precipitation method and study of their photocatalytic activity in the degradation of rhodamine B. Biomass Conversion and Biorefinery. 2022;14(3):3477-3487.
57. Al-Asadi ST, Al-Qaim FF. Adsorption of Methylene Blue Dye from aqueous solution using low cost adsorbent: Kinetic, Isotherm Adsorption and Thermodynamic Studies. Research Square Platform LLC; 2023.
58. Pulat M, Çetin M. Pantoprazole-Na Release from Poly(acrylamide-co-crotonic acid) and Poly(acrylic acid-co-crotonic acid) Hydrogels. Journal of Bioactive and Compatible Polymers. 2008;23(4):305-318.
59. Azhar-ul-Haq M, Javed T, Abid MA, Masood HT, Muslim N. Adsorptive removal of hazardous crystal violet dye onto banana peel powder: equilibrium, kinetic and thermodynamic studies. Journal of Dispersion Science and Technology. 2022:1-16.
60. Gopal V, Elango KP. Equilibrium, kinetic and thermodynamic studies of adsorption of fluoride onto plaster of Paris. Journal of Hazardous Materials. 2007;141(1):98-105.
61. Shakerimoghaddam A, Majeed HJ, Hashim AJ, Abed MJ, Jasim LS, Salavati-Niasari M. Green synthesis and characterization of NiO/Hydroxyapatite nanocomposites in the presence of peppermint extract and investigation of their antibacterial activities against Pseudomonas aeruginosa and Staphylococcus aureus. Results in Chemistry. 2025;13:101947.